ELSEVIER

Journal of Photochemistry and Photobiology A: Chemistry 153 (2002) 25–31

Journal of Photochemistry and Photobiology A:Chemistry

www.elsevier.com/locate/jphotochem

Kinetics of thermal decoloration of a photomerocyanine in mixtures of protic and nonpolar solvents

Germán Sciaini [a], Diana E. Wetzler [a], Jorge Alvarez [b,c], Roberto Fernández-Prini [a,b], María Laura Japas [b,d,*]

[a] *INQUIMAE, Facultad de Ciencias Exactas y Naturales, Universidad de Buenos Aires, Ciudad Universitaria, Pabellón 2, 1428-Buenos Aires, Argentina*
[b] *Unidad Actividad Química, Comisión Nacional de Energía Atómica, Av. Libertador 8250, 1429-Buenos Aires, Argentina*
[c] *Dpto. Ingeniería Química, FRBA, Universidad Tecnológica Nacional, Medrano 951, 1179-Buenos Aires, Argentina*
[d] *Escuela de Ciencia y Tecnología, Universidad Nacional de San Martín, Alem 3901, 1653-Villa Ballester, Province Buenos Aires, Argentina*

Received 6 June 2002; received in revised form 20 July 2002; accepted 22 July 2002

Abstract

The kinetics of thermal conversion of a photogenerated merocyanine into its more stable spiropyrane form was studied in mixtures of ethanol with nonpolar solvents, toluene, *n*-hexane or CO_2. For solutions of ethanol concentration higher than ca. 1.5 M two decay rates are observable. Below that concentration, the relative amplitude of the slow mode becomes negligible, compared to the fast, and the observed kinetics is monoexponential. As reported before in toluene–acetonitrile mixtures, the rate constant for the thermal decay in toluene–ethanol passes through a shallow maximum at low-ethanol concentrations. The activation energy and entropy of both processes were determined; the data corresponding to the fast process have a complex alcohol concentration dependence. A three-species reaction scheme proposed previously for neat alcohols, supplemented with an approximation regarding the effect of medium polarity on the assumed species, is able to capture the essential features of all activation thermodynamic functions in the studied mixtures.
© 2002 Elsevier Science B.V. All rights reserved.

Keywords: Kinetics; Thermal decoloration; Photomerocyanine

1. Introduction

Spiropyranes (SP) are compounds which photoisomerize when irradiated with UV; the resulting photoisomer is a merocyanine (MC) that absorbs visible light. MC reverts to the stable SP isomer by thermal or photochemical processes. The kinetics of the thermal bleaching is strongly influenced by the medium [1–7]; the rate constant of the dark conversion of MC into SP decreases as the polarity of the solvent increases. Moreover the logarithm of that rate constant was found to be linearly related to the wavelength of the absorption maximum of MC in the visible range [2]. The fact that these two quantities increase with decreasing solvent polarity was interpreted as an indication of the lower dipole moment of the transition and the excited states of MC compared with the ground state [8–10].

In pure solvents, the thermal decoloration of MC was found to be monoexponential in nonpolar (np) and aprotic polar (ap) solvents, while doubly exponential in protic polar (pp) solvents, with two rate constants that characterize a fast (f) and a slow (s) kinetic processes [11,12]. The corresponding activation energies were found to be typically 70–80 kJ mol^{-1} in nonpolar solvents and around 100 kJ mol^{-1} in aprotic polar media [2]. In protic polar solvents, the values found for the activation energy of the fast process were similar to those obtained for nonpolar solvents, while for the slow process they were close to the values in aprotic polar solvents [11].

In a previous work we have studied [11] the effect of the medium on the kinetics of the thermal bleaching of the merocyanine form of 6-nitro benzospiropyran (6-nitroBIPS), in both nonpolar–aprotic (np–ap) and nonpolar–protic (np–pp) solvent mixtures. For np–ap mixtures the kinetics was found to be monoexponential over the whole composition range of the solvent mixture, while for np–pp solvent mixtures a monoexponential behavior was only encountered at low concentrations of the protic solvent component; at higher pp concentrations double exponential decays were observed. An interesting observation reported in [11] for np–ap systems was that the rate constant of decoloration of MC passed through a maximum for mixtures that were very dilute in the ap component, implying that polarity and rate constant are not monoton-

* Corresponding author.
E-mail address: mljapas@cnea.gov.ar (M. Laura Japas).

1010-6030/02/$ – see front matter © 2002 Elsevier Science B.V. All rights reserved.
PII: S1010-6030(02)00294-0

ically related in solvent mixtures over that composition range.

The activation energies for np–ap mixtures were found to change abruptly from typical np to typical ap values as the concentration of the ap component was increased approximately above 0.5 M. For np–pp mixtures, the activation energy at low pp concentration (corresponding to the monoexponential behavior) was close to 100 kJ mol^{-1}; for higher pp concentrations the activation energies of the fast and slow processes were in general those of pure np and ap systems, respectively. The entropy of activation showed a similar trend with no indication of diffusional relaxation in the transition state.

The aim of the present work was to improve our understanding of the kinetic behavior of the MC thermal decay in nonpolar-ethanol (np-EtOH) mixtures by analyzing the experimental results in terms of the model proposed by Bertelson [12] for the thermal decay of MC in neat alcohols. To achieve this purpose the kinetic data obtained in our previous study were complemented with new results in the low-ethanol solvent composition range. The new experimental data for the kinetics of the MC thermal decoloration were obtained in binary solvent mixtures of toluene (Tol), supercritical CO_2 and *n*-hexane (Hex) with ethanol. The first mixture allowed us to study the very low ethanol concentration range where an anomalous relation between polarity and kinetics has been reported, without the interference of dimer formation. Supercritical CO_2 with ethanol as cosolvent was used because it was expected that in this medium preferential solvation by ethanol would be enhanced [13]. In order to combine these results with those of our previous study, we have also measured in the present work the kinetics of MC decoloration in mixtures of Hex–EtOH at intermediate ethanol concentration over a temperature range.

2. Experimental

2.1. Chemicals

1′,3′-Dihydro-1′,3′,3′-trimethyl-6-nitrospiro[2*H*-1-benzopyran-2,2′-(2*H*)-indole], the spiropyrane SP used in this work (Aldrich), the liquid solvents toluene (Merck, Uvasol), *n*-hexane (Merck, p.a.) and absolute ethanol (Merck, p.a.), and carbon dioxide (AGA, 99.9%) were all used as received.

2.2. Kinetic measurements

Depending on the type of solvent mixtures that were studied, two different set-ups were used to photolyse the SP. For the liquid mixtures Tol–EtOH and Hex–EtOH the samples, placed in a 1 cm × 1 cm quartz cuvette, were photolysed with a photography flash whose plastic cover had been removed. The solvent mixtures with CO_2, contained in a high-pressure vessel, were irradiated with a metal halide lamp (Osram, 250 W). The beam was attenuated by a water filter, to absorb the IR radiation from the lamp, reducing the heating of the sample, and by an appropriate cut-off filter (UG1, Schott Glass, Germany) in order to block the visible wavelengths that induce the photobleaching of MC. Pressure was measured with a pressure transducer (Burster, precision of 0.1% full scale) that was calibrated against a deadweight balance (Ruska).

The optical cell, either the high-pressure one or the quartz cuvette, was placed in a thermostated holder. Temperature was regulated to ±0.1 K by fluid circulation from a thermostat and measured in the optical cell with a calibrated thermistor during the measurement. The kinetics of the thermal decoloration was followed measuring the absorbance at fixed wavelength (500–600 nm, the maximum wavelength of the absorption of MC), as a function of time in a Shimadzu PC3100 spectrophotometer.

2.3. Preparation of solvent mixtures

Liquid solvent mixtures were prepared by adding the nonpolar solvent component to a well-measured volume of ethanol at room temperature. The solvent mixtures containing CO_2 were prepared in situ, injecting known amounts of CO_2 with a calibrated hand-pump into a high-pressure optical cell containing predetermined quantities of ethanol. In the preparation of the solvent mixture CO_2–EtOH care was taken to avoid the formation of two fluid phases [14–16]. The volume of the cell was calibrated, in this way the molar composition of the ethanol and CO_2 in the mixture could be accurately calculated.

The conditions at which CO_2–EtOH mixtures could be used were dictated by the system's properties. SP has been reported [17] to form dimers in supercritical CO_2 as is the case in neat hexane, thus hampering the study of the kinetics of decoloration of MC in pure CO_2. On the other hand, the temperature range was limited by the fact that, at high temperatures, the processes leading to the decoloration of MC become too fast to allow us to measure their rates. Due to the low solubility of the probe molecule in CO_2 at low fluid density and to an upper pressure limit of 20 MPa for safe operation of the spectrophotometric cell, the density range was restricted between 14.5 and 22 mol dm^{-3}, i.e. at supercritical temperatures the solvent mixture was an expanded liquid.

The total concentration of SP was always kept smaller than 10^{-4} M. Kinetic runs were done for temperatures between 284 and 322 K.

3. Results

For solvent mixtures having an ethanol concentration $c_{EtOH} > 1.5$ M the kinetics were biexponential, the time dependence of the solutions' optical absorbance of MC $a(t)$ at

Table 1
Arrhenius parameters for the thermal decoloration of MC in carbon dioxide–ethanol mixtures

c_{EtOH} (M)	E_{af} (kJ mol^{-1})	ln(A_f) (s^{-1})	E_{as} (kJ mol^{-1})	ln(A_s) (s^{-1})	ΔT[a] (K)
0.47[b]	94	36.6	–	–	[284–289]
0.94	83	31.0	–	–	[279–293]
1.89	92	34.2	83	27.7	[288–312]
2.83	91	33.3	91	31.3	[289–322]
3.77	87	31.7	95	32.8	[294–317]
4.72	84	30.4	103	35.9	[289–306]

[a] Temperature range.
[b] At this concentration only two temperatures could be studied.

the wavelength of the maximum could be well described by

$$a(t) = a_f \exp(-k_f t) + a_s \exp(-k_s t) \quad (1)$$

where subscripts f and s denote the fast and slow processes, respectively. For $c_{EtOH} < 1.5$ M Eq. (1) did not fit the data well because a_s was too small (vide infra) and the resulting parameters for the slow process were meaningless. To obtain a more precise value of the kinetic parameters of the fast process for these solvent mixtures we adjusted the kinetic data to Eq. (1), but disregarded the values of a_s and k_s for these mixtures. Within the limited range of fluid density that could be covered in this work, merocyanine dissolved in CO_2–EtOH mixtures did not show any significant dependence of the spectrum and of the kinetics of decoloration on fluid density.

The ln k_i values were linearly dependent on T^{-1}, the Arrhenius plots for all the solvent mixtures yielded the values of the activation energies, E_{ai}, for the fast and the slow processes. The entropy of activation was determined using the values of the rate constants and the calculated activation energies. Table 1 reports the values of the kinetic parameters for the MC decoloration in CO_2–EtOH mixtures; it should be remarked that E_a for the lowest c_{EtOH} is only an estimate because the temperature range covered for this solvent mixture was limited to low temperatures where the decay occurred at a rate which could be followed with precision in our set-up. Tables 2 and 3 report the kinetic parameters in Hex–EtOH and Tol–EtOH solvent mixtures, respectively. In the last columns of the three tables the temperature range covered in the measurements is given.

Fig. 1 shows the plots of ln k_i against c_{EtOH} at 298 K for the three solvent mixtures and it includes data from our previous study [11]. The datum for the lowest c_{EtOH} in CO_2–EtOH mixtures plotted in Fig. 1 was extrapolated at 298 K with the parameters obtained at lower temperature.

Table 2
Arrhenius parameters for the thermal decoloration of MC in hexane–ethanol mixtures

c_{EtOH} (M)	E_{af} (kJ mol^{-1})	ln(A_f) (s^{-1})	E_{as} (kJ mol^{-1})	ln(A_s) (s^{-1})	ΔT[a] (K)
0.34	98	37.2	–	–	[283–308]
0.81	95	35.5	–	–	[283–313]
1.70	92	33.4	98	32.8	[283–323]

[a] Temperature range.

Table 3
Arrhenius parameters for the thermal decoloration of MC in toluene–ethanol mixtures

c_{EtOH} (M)	E_{af} (kJ mol^{-1})	ln(A_f) (s^{-1})	E_{as} (kJ mol^{-1})	ln(A_s) (s^{-1})	ΔT[a] (K)
0.017	63	23.0	–	–	[280–305]
0.17	88	33.4	–	–	[285–307]
1.7	81	29.5	100	34.7	[285–307]

[a] Temperature range.

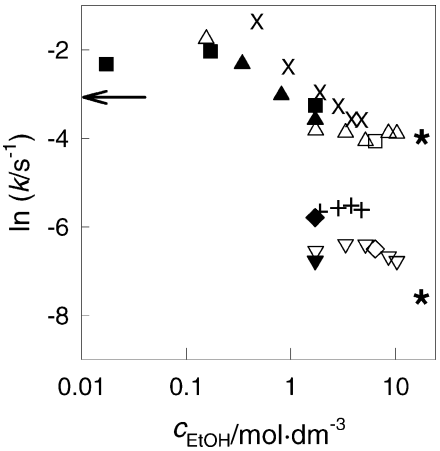

Fig. 1. Experimental ln k_i at 298 K for all studied systems containing ethanol, as a function of the molar concentration of ethanol. (X) k_f and (+) k_s in CO_2–EtOH; (▲) k_f and (▼) k_s in Hex–EtOH; (■) k_f and (◆) k_s in Tol-EtOH. Values for pure ethanol are indicated with stars (✱). The arrow indicates the value of ln(k_f) for MC dissolved in pure toluene. Open symbols have the same meaning, but were taken from [11].

4. Discussion

4.1. Rate constants

The first issue to be addressed is the dependence of the kinetic behavior on the concentration of ethanol in the solvent mixtures. The disappearance of one of the two decay processes as the alcohol concentration decreases, could be due to changes in the relative values of the amplitudes or to a shift of the characteristic times so that they become very similar [11]. In order to obtain reasonable estimates of the amplitudes for the two processes in the CO_2–EtOH mixtures, appropriate values for the time elapsed between sample irradiation and the first possible measurement of optical absorption were estimated. The calculated ratios a_s/a_f for runs below room temperature are plotted in Fig. 2 as a function of c_{EtOH}; the ratio did not depend critically on the temperature, but results for higher temperatures were not included because the amplitude of the fast process had larger uncertainty due to the concomitant increase in the rate of reaction.

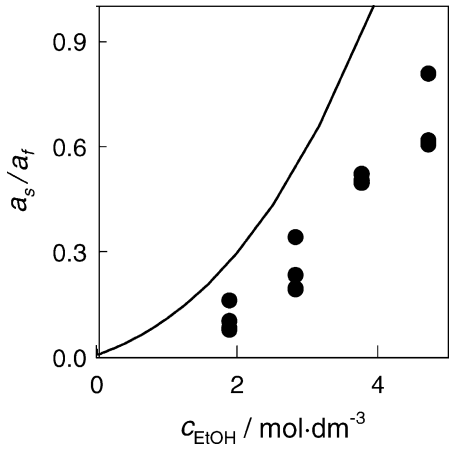

Fig. 2. Ratio of amplitudes of the slow (a_s) to the fast (a_f) processes for CO_2–EtOH mixtures at 298 K. Points: experimental results; curve: calculated with the three-species model (see text).

Fig. 2 shows clearly that the reason for the change in the kinetic law followed by the MC thermal decay as the ethanol concentration increases, monoexponential at low c_{EtOH} and biexponential at high c_{EtOH}, is that the amplitude of the *slow* process becomes too small at low c_{EtOH} to contribute significantly to the total time dependence of the decoloration of the dye molecule. Therefore, it is possible to rule out the coincidence in the rate constants of both processes as a cause for the monoexponential decay at low c_{EtOH}. Consequently, all the rate constants obtained here and in the previous paper [11] for np-EtOH mixtures at low alcohol concentration should be assigned to the fast process.

In our previous study [11] it was noted that in toluene–acetonitrile (Tol–Acn) mixtures, for Acn concentrations lower than ca. 0.5 M, ln k did not depend monotonously on the polarity of the solvent mixtures, as measured by the solvatochromic effect of the medium on $E_T(30)$, [18]. The effect, although small, is above the level of experimental uncertainty. In the present study we have observed the same behavior for np-EtOH mixtures having $c_{EtOH} < 0.2$ M, that is the rate constant of the fast process increases with c_{EtOH}. This verification was only possible in solvent mixtures having toluene as the np component, in all the other nonpolar solvents used dimers of MC are formed when c_{EtOH} is very low.

A qualitative characterization of the kinetics of MC thermal decay in np-EtOH mixtures for different ranges of c_{EtOH}, defines three distinctive regions:

- Region a, c_{EtOH} < ca. 0.2 M: Only one decay process is observed, its rate constant k_f increases with the polarity of the medium, an *inverse* behavior with respect to what has been observed for neat solvents with increasing polarity. As mentioned before, this region could only be studied in Tol–EtOH mixtures.
- Region b, corresponding to ca. 0.2 < c_{EtOH} < 1.5 M: Still a single exponential decay was observed. The values of k_f are affected by the polarity of the medium in a *normal* way, decreasing k_f with increasing polarity.
- Region c, $c_{EtOH} > 1.5$ M: There are two rate constants for the biexponential MC thermal decay: k_f does not depend, within the experimental uncertainty, on the medium polarity while k_s passes through a flat maximum and finally decreases with increasing alcohol concentration.

In regions a and b of np-EtOH mixtures, the only rate constant that is observable, i.e. the rate constant of the *fast* process k_f, shows the same general trends as the rate constant in Tol–Acn; in region c however the dependence of k_f on c_{EtOH} changes and, simultaneously, a second process emerges. This observation strongly suggests that the appearance of the slow process and the insensitivity of the fast process to the polarity of the medium are related.

After the qualitative characterization of the dependence of rate constants on c_{EtOH} it is worthwhile to establish if this qualitative description is supported by the simplest possible model for the kinetic process. The main reason for proposing this model for the observed kinetic behavior has been to shed light into the different kinetic behaviors observed in np–ap and np–pp solvent mixtures, hence we do not expect that the simple model will enable us to describe the behavior in region a. We have used a mechanism proposed by Bertelson to explain the thermal decay of MC in neat alcohols, [12] it assumes that two photoisomers of MC are generated, one of them is colored (C) and the other uncolored (U). The reaction scheme may be depicted by

$$U \underset{k_1}{\overset{k_2}{\rightleftarrows}} C \xrightarrow{k_3} SP$$

The corresponding kinetic equations and the solution for the concentration time dependence of the colored species C are [12]

$$\frac{d[C]}{dt} = -(k_1 + k_3)[C] + k_2[U]$$

$$\frac{d[U]}{dt} = k_1[C] - k_2[U]$$

$$\frac{d[SP]}{dt} = k_3[C]$$

$$[C] = a_f \exp(-k_f t) + a_s \exp(-k_s t) \quad (2)$$

where k_f and k_s in terms of the elementary rate constants k_1 to k_3 are given by

$$k_i = \tfrac{1}{2}(k_1 + k_2 + k_3) \pm \tfrac{1}{2}[(k_1 + k_2 + k_3)^2 - 4k_2k_3]^{1/2} \quad (3)$$

the positive sign corresponds to the fast process and the negative to the slow process. In order to analyze the observed trends, it is convenient to combine Eq. (3), to yield

$$k_+ = k_s + k_f = k_1 + k_2 + k_3 \quad (4)$$

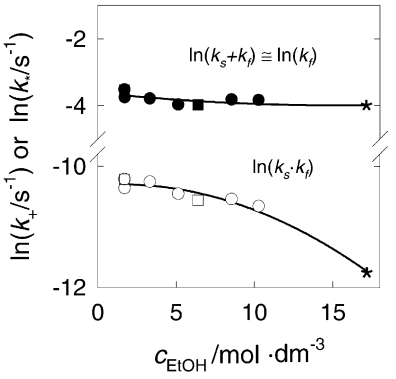

Fig. 3. Experimental results of $\ln(k_+) = \ln(k_s + k_f)$ (full symbols), and $\ln(k_*) = \ln(k_s k_f)$ (open symbols) for biexponential decay in Tol–EtOH (squares) and Hex–EtOH (circles) mixtures at 298 K as a function of the molar concentration of ethanol. Values for neat ethanol are indicated with stars (★).

$$k_* = k_s k_f = k_2 k_3 \tag{5}$$

k_+ and k_* are preferred to k_f and k_s because they simplify the relations between empirical and elementary rate constants (Eqs. (4) and (5) and Eq. (3), respectively). Fig. 3 depicts the experimental dependence of k_+ and of k_* on c_{EtOH} for Tol–EtOH and Hex–EtOH mixtures.

The interpretation of the data for mixtures of nonpolar fluids and ethanol in terms of the three-species model requires information on the dependence of the k_1 to k_3 on the alcohol concentration. The step representing the direct conversion of the colored form into the stable SP isomer (step 3) should exhibit the same behavior as in np–ap solvent mixtures since the species involved are the same, i.e. ground (colored) and excited states of MC. However, there is no information about the dependence on the medium polarity of k_1 and k_2. To apply the proposed mechanism to the present data, some assumptions have to been made.

In the pure-alcohol limit ($c_{EtOH} = 17.1\,\text{mol dm}^{-3}$), $\ln(k_+ (\text{s}^{-1})) \approx -4.0$ and $\ln(k_* (\text{s}^{-1})) \approx -11.75$ (see Fig. 3). The polarity dependence of k_3 was obtained by fitting the rate constants of several pure nonpolar and aprotic polar solvents [7] to a straight line ($\ln(k_{298\,K} (\text{s}^{-1})) = 7.88 - 0.0717$ ($E_T(30)$ (kJ mol^{-1})), regression coefficient 0.97). Using this result, a value of $\ln k_3 \approx -7.75$ was calculated for pure ethanol ($E_T(30)_{EtOH} = 218\,\text{kJ mol}^{-1}$ at 298 K). Therefore, according to Eq. (5), for solutions of MC in *neat ethanol*, $\ln k_2 \approx -11.75 - \ln k_3 = -4$, so that $k_+ \approx k_2$. This implies that in *neat ethanol* k_3 and k_1 are both much smaller than k_2.

In np-EtOH mixtures, the constancy of k_+ over the entire c region, $1.5\,\text{mol dm}^{-3} < c_{EtOH} < 17.1\,\text{mol dm}^{-3}$ (see Fig. 3) should therefore be interpreted as an indication that k_2 remains unchanged in that region, disregarding a less likely situation involving a fortuitous cancellation of effects. Since k_2 is related to the difference of Gibbs energy between the transition state $T_1^{\ddagger}$ and

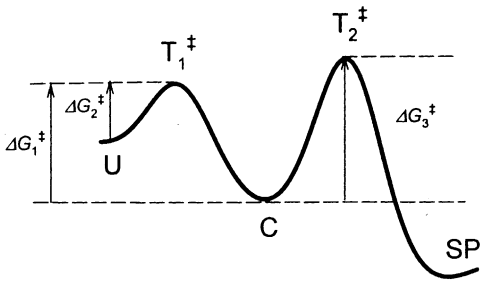

the ground state of photoisomer U, np-EtOH data indicate that both states have a very similar, although unknown, medium polarity dependence.

For Hex–EtOH and Tol–EtOH, where the experimental information is more abundant, we have explored two possible situations. In the first one, we have assumed that neither U nor $T_1^{\ddagger}$ have a large dipole moment, hence we have neglected the dependence of their energy on polarity; this implies that the effect of medium polarity is restricted only to the energy of photoisomer C. Thus, the difference between $\Delta^* G_1$ and $\Delta^* G_3$ is a constant and k_1 will be proportional to k_3 independently of the concentration of the polar solvent component. A second possibility is that both U and $T_1^{\ddagger}$ change their energies with the medium polarity, but that they change in a similar way to keep k_2 constant. In this case the c_{EtOH} dependence of k_1 and k_3 would be uncoupled. Both possibilities were evaluated in their capacity to represent the experimental rate constants. The second, more general picture, gave unphysical results when leaving all adjustable parameters unconstrained, e.g. the value of k_3 had a polarity dependence opposite to that observed experimentally. However, forcing k_3 to decrease with polarity, but letting its absolute value free, also yielded values of k_1 that were proportional to those of k_3. Consequently we adopted the simplest hypothesis involved in the first situation.

We have fitted k_s and k_f with this model using our results in the Hex–EtOH solvent mixture at 298 K where we have kinetic data over a wider c_{EtOH} range. The dependence of k_3 on ethanol concentration was represented by a polynomial with three coefficients. Fig. 4a shows the curves obtained by fitting the Hex–EtOH data to the model. The agreement between experimental and calculated k_s and k_f is fair over all the range of ethanol concentration; the simple model is able to capture the observed features in np–pp solvent mixtures. It is interesting to note that the values of k in Tol–Acn [11] follow a curve roughly parallel to k_3 (or k_1) (see Fig. 4a). The similar polarity dependence between the experimental rate constant k in Tol–Acn, presumed single-step, and the adjusted model-dependent rate constant k_3, supports the scheme proposed for mixtures containing ethanol because both describe the kinetics of the same elementary reaction, colored-MC → SP.

The simple three-species model can also be used to describe the rate constants of MC dissolved in CO_2–EtOH, as shown in Fig. 4b. Compared with the values obtained

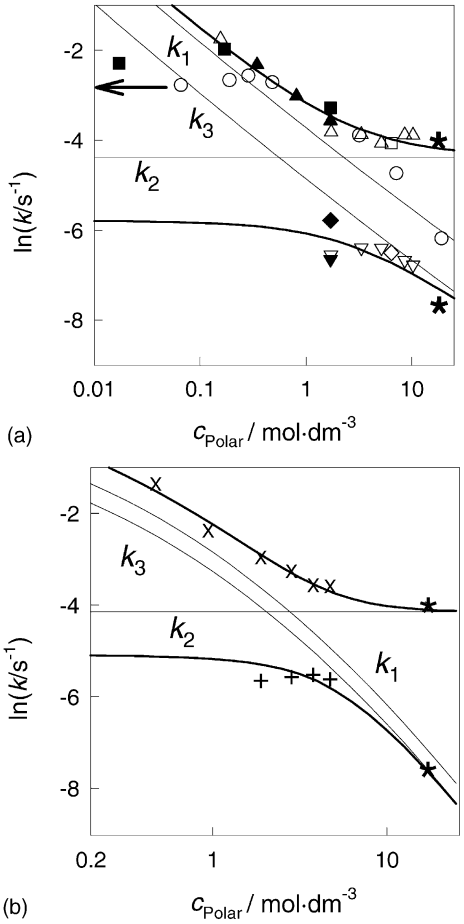

Fig. 4. (a) $\ln k_i$ at 298 K for the liquid solvent mixtures as a function of the molar concentration of the polar liquid solvent. Symbols and arrow have the same meaning than in Fig. 1. For comparison, previous results of k in Tol–Acn (○) are shown. Thin curves: calculated values of k_f and k_s for Hex–EtOH system obtained by nonlinear fitting of the experimental data to Eq. (2); thick lines: rate constants of the elementary steps 1–3. (b). $\ln k_i$ at 298 K for the CO_2–EtOH mixtures as a function of the molar concentration of the polar liquid solvent. Symbols have the same meaning than in Fig. 1. Thick lines: calculated values of k_f and k_s obtained by nonlinear fitting of the experimental data to Eq. (2); thin lines: rate constants of the elementary steps 1–3.

in Tol–EtOH, k_2 remains almost unchanged and k_1 shows a slightly different concentration dependence. According to this model, the observed increase in the rate constants of the slow process in CO_2–EtOH compared with those in the Tol–EtOH solvent mixture are consequence of the relative increase of k_3, which for CO_2–EtOH is closer to k_1.

Despite the simplicity of the model and the approximations made to reduce the number of adjustable parameters, the decomposition of the empirical rate constants k_f and k_s in terms of the rate constants of the elementary steps gives an interesting interpretation of some observations. The different polarity dependence of k_f at low and high alcohol concentration originates in the fact that the curves of k_1 and k_2 cross each other when the ethanol concentration increases. According to Eq. (4), k_f is always larger than any of the elementary-step rate constants k_i—independently of the approximations about their polarity dependence. Therefore, as c_{EtOH} increases, k_f changes from being parallel to k_1 to following k_2 when this rate constant becomes larger than k_1.

The amplitudes of the fast and the slow processes, a_f and a_s respectively, can be calculated with the simple model using the equations derived in [12], if the initial concentrations of species U and C are known. The concentration of species U could not be measured, nevertheless it was possible to assume that U is not generated in significant amount by the photochemical reaction because the kinetics were identical when SP was irradiated before or after the addition of ethanol to the solvent, and under no conditions the concentration of C was observed to increase with time. The calculated ratio (a_s/a_f) for CO_2–EtOH mixtures, plotted as a curve in Fig. 2, is in qualitative agreement with the experimental data.

The simple mechanism offers also a means of relating the amplitudes of two elementary decay processes with the rate constants. Making use of our assumptions, we obtain

$$\frac{a_s}{a_f} \approx \frac{k_f}{k_1} - 1 \qquad (6)$$

which explains the coupling between the insensitivity of k_f on polarity and the appearance of the slow process: in regions a and b, k_f is close to k_1 and therefore a_s/a_f is almost zero, while in region c, $k_f \approx k_2 > k_1$ and larger values of a_s/a_f are obtained.

4.2. Activation energies

The activation energy E_{af} of the fast process shows a complex dependence on the alcohol concentration, as illustrated in Fig. 5a. In region a, E_{af} for Tol–EtOH increases very steeply with c_{EtOH}, from 60 to 70 kJ mol^{-1} in neat toluene to near 90 kJ mol^{-1} at $c_{EtOH} = 0.17$ M. In the b region, E_{af} changes with ethanol concentration according to the expected effect of the medium polarity decreasing smoothly with the concentration of alcohol to reach finally, at $c_{EtOH} \approx 3$ M (region c), a constant value which is very close to the typical value of E_a in np solvents. The activation energy of the slow process, represented in Fig. 5b, increases with polarity and also reaches a plateau at about the same c_{EtOH} when $E_{as} \approx 110$ kJ mol^{-1}, a value typical in pure ap solvents. The curves drawn in Fig. 5 were calculated with the simple model for the reaction mechanism.

The results obtained in CO_2–EtOH mixtures, also plotted in Fig. 5, are consistent with those observed in Hex–EtOH and Tol–EtOH mixtures, although the curves calculated with the simple model for the fast and slow processes seem to be shifted to higher alcohol concentration. This fact is opposite to what was expected from the enhanced preferential solvation phenomena displayed in supercritical fluids [19].

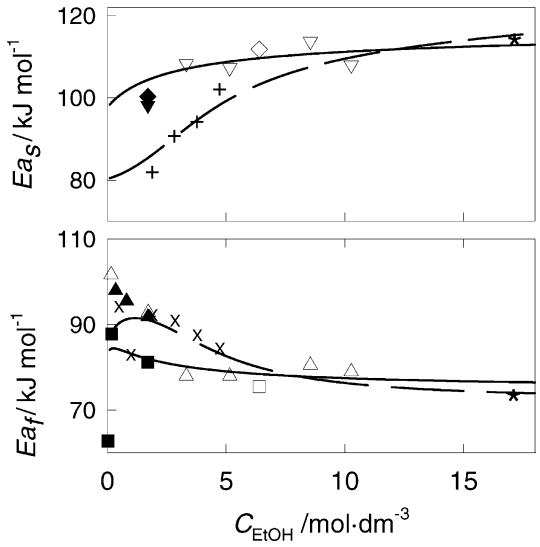

Fig. 5. Activation energy for the fast (lower panel) and slow (upper panel) processes. Symbols have the same meaning as in Fig. 1. Full curves: Hex–EtOH and Tol–EtOH mixtures; dashed curves: CO_2–EtOH, all of them calculated with the simple mechanism.

It is worth mentioning that all data for CO_2–EtOH mixtures correspond to densities higher than the critical density, but that, compared to the liquid solvents, the systems containing CO_2 were expanded fluids in which repulsions have less importance than in close packed fluids.

The entropy of activation of both processes in all studied systems mimics the behavior displayed by the corresponding activation energy. $\Delta S_f^{\ddagger}$ goes from the pure toluene value to $\Delta S_f^{\ddagger}$ in neat ethanol (around $-40\,J\,mol^{-1}\,K^{-1}$) for both cases) by first increasing to a maximum (ca. $+50\,J\,mol^{-1}\,K^{-1}$) to then decrease. For the slow process the entropy of activation is a monotonously increasing function of the alcohol concentration, as is E_{as}. As reported before, [11] the thermodynamic parameters of activation E_a and $\Delta S^{\ddagger}$ show a strong linear correlation.

5. Conclusions

The results of this study show that the change in the thermal decay rate law with c_{EtOH} is due to the very low amplitude of the *slow* process when c_{EtOH} is small. The three-species model is able to describe the general behavior of the np-EtOH systems: the change in polarity dependence of the rate constant k_f and the concomitant appearance of a second process. The rate constants in the supercritical solvent mixture CO_2–EtOH exhibit similar trends as those found for Tol–EtOH or Hex–EtOH. Surprisingly, these results show no indication of preferential solvation of MC by ethanol in the expanded fluid CO_2.

The origin of the behavior in the inverse region remains unclear; other factors besides polarity may play a role in this region.

Acknowledgements

The authors are very grateful to Dr. Pedro Aramendía for valuable discussions and critical reading of the manuscript. Partial economic support by ANPCyT and UBACyT are acknowledged. RFP is member of Carrera del Investigador Científico (CONICET, Argentina).

References

[1] R. Guglielmetti, in: H. Dürr, H. Bouas-Laurent (Eds.), Photochromism, Molecules and Systems, Elsevier, Amsterdam, 1990, Chapter 8.
[2] Y. Sueishi, M. Ohcho, N. Nishimura, Bull. Chem. Soc. Jpn. 58 (1985) 2608.
[3] (a) N.P. Ernsting, B. Dick, Th. Arthen-Engeland, Pure Appl. Chem. 62 (1990) 1483;
(b) N.P. Ernsting, Th. Arthen-Engeland, J. Phys. Chem. 95 (1991) 5502.
[4] (a) H. Görner, L.S. Atabekyan, A.K. Chibisov, Chem. Phys. Lett. 260 (1996) 59;
(b) A.K. Chibisov, H. Görner, J. Photochem. Photobiol. A: Chem. 105 (1997) 261;
(c) H. Görner, Chem. Phys. 222 (1997) 315;
(d) A.K. Chibisov, H. Görner, J. Phys. Chem. A 101 (1997) 4305.
[5] (a) F. Wilkinson, D.R. Worrall, J. Hobley, L. Jansen, S.L. Williams, A.J. Langley, P. Matousek, J. Chem. Soc., Faraday Trans. 92 (1996) 1331;
(b) J. Hobley, F. Wilkinson, J. Chem. Soc., Faraday Trans. 92 (1996) 1323.
[6] J.Z. Zhang, B.J. Schwartz, J.C. King, C.B. Harris, J. Am. Chem. Soc. 114 (1992) 10921.
[7] J.T.C. Wojtyk, A. Wasey, P.M. Kazmaier, S. Hoz, E. Buncel, J. Phys. Chem. A 104 (2000) 9046.
[8] M. Levitus, G. Glasser, D. Neher, P.F. Aramendía, Chem. Phys. Lett. 277 (1997) 118.
[9] D. Lapienis-Grochowska, M. Kryszewsky, B. Nadolski, J. Chem. Soc., Faraday Trans. 2 75 (1979) 312.
[10] (a) J. Zhou, Y. Li, Y. Tang, F. Zhao, X. Song, E. Li, J. Photochem. Photobiol. A 90 (1995) 117;
(b) X. Song, J. Zhou, Y. Li, Y. Tang, J. Photochem. Photobiol. A 92 (1995) 99.
[11] D.E. Wetzler, P.F. Aramendía, M.L. Japas, R. Fernández-Prini, Phys. Chem. Chem. Phys. 1 (1999) 4955.
[12] R.C. Bertelson, in: G.H. Brown (Ed.), Techniques in Chemistry: Photochromism, vol. 3, Wiley/Interscience, New York, 1971.
[13] D. Laría, M.S. Skaf, J. Chem. Phys. 111 (1999) 300.
[14] K. Suzuki, H. Sue, M. Itou, R.L. Smith, H. Inomata, K. Arai, S. Saito, J. Chem. Eng. Data 35 (1990) 63.
[15] D.W. Jennings, R.-J. Lee, A.S. Teja, J. Chem. Eng. Data 36 (1991) 303.
[16] J.-H. Yoon, H.-S. Lee, H. Lee, J. Chem. Eng. Data 38 (1993) 53.
[17] Y. Kimura, Y. Takebayashi, H. Hirota, J. Phys. Chem. 100 (1996) 11009.
[18] C. Reichardt, Chem. Rev. 94 (1994) 2319.
[19] O. Kajimoto, Chem. Rev. 99 (1999) 355.